Published in final edited form as:
J Chem Neuroanat. 2011 October ; 42(2): 118–126. doi:10.1016/j.jchemneu.2011.06.007.

Microarray analyses of laser-captured hippocampus reveal distinct gray and white matter signatures associated with incipient Alzheimer's disease

Eric M. Blalock[a,*], **Heather M. Buechel**[a], **Jelena Popovic**[a], **James W. Geddes**[b], and **Philip W. Landfield**[a]

[a] Department of Molecular and Biomedical Pharmacology, University of Kentucky College of Medicine, Lexington Kentucky

[b] Spinal Cord and Brain Injury Research Center, University of Kentucky College of Medicine, Lexington Kentucky

Abstract

Alzheimer's disease (AD) is a devastating neurodegenerative disorder that threatens to reach epidemic proportions as our population ages. Although much research has examined molecular pathways associated with AD, relatively few such studies have focused on the disease's critical early stages. In a prior microarray study we correlated gene expression in hippocampus with degree of Alzheimer's disease and found close associations between upregulation of apparent glial transcription factor/epigenetic/tumor suppressor genes and incipient AD. The results suggested a new model in which AD pathology spreads along myelinated axons (Blalock *et al*., 2004). However, the microarray analyses were performed on RNA extracted from frozen hand-dissected hippocampal CA1 tissue blocks containing both gray and white matter, limiting the confidence with which transcriptional changes in gray matter could be distinguished from those in white matter. Here, we used laser capture microdissection (LCM) to exclude major white matter tracts while selectively collecting CA1 hippocampal gray matter from formalin-fixed, paraffin-embedded (FFPE) hippocampal sections of the same subjects assessed in our prior study. Microarray analyses of this gray matter-enriched tissue revealed many transcriptional changes similar to those seen in our past study and in studies by others, particularly for downregulated neuron-related genes. Additionally, the present analyses identified several previously undetected pathway alterations, including downregulation of molecules that stabilize ryanodine receptor Ca2+ release and upregulation of vasculature development. Conversely, we found a striking paucity of the upregulated changes in the putative glial and growth-related genes that had been strongly overrepresented in the prior mixed-tissue study. We conclude that FFPE tissue can be a reliable resource for microarray studies of brain tissue, that upregulation of growth-related epigenetic/transcription factors during incipient AD is predominantly localized in and around white matter (supporting our prior findings and model), and that novel alterations in vascular and ryanodine receptor-related pathways in gray matter are closely associated with incipient AD.

[*] to whom correspondence should be addressed MS-309, Department of Molecular and Biomedical Pharmacology University of Kentucky College of Medicine 800 Rose Street Lexington, KY 40536 Phone: 859 323-8033 Fax: 859 323-1945 emblal@uky.edu .

[1]Abbreviations: AD- Alzheimer's disease; CA- *Cornu Ammonis*; FFPE: Formalin-fixed, paraffin-embedded; LCM- laser capture microdissection; MMSE- mini-mental status exam; NFT- neurofibrillary tangle

Keywords

Cognitive impairment; ageing; neurodegeneration; neurofibrillary tangles; myelin; glia

1. Introduction

The major pathological hallmarks of Alzheimer's disease (AD) include beta amyloid accumulation (Hardy and Selkoe, 2002; Klein *et al*., 2001; Morgan, 2003; Mucke *et al*., 2000; Mullan and Crawford, 1994; Price and Sisodia, 1998; Tanzi and Bertram, 2001), neurofibrillary tangles (NFTs) (Davies and Koppel, 2009; Johnson and Bailey, 2002; Morris *et al*., 2011; Noble *et al*., 2003) and synaptic dysfunction or loss (Masliah *et al*., 1994; Scheff and Price, 2001; Sze *et al*., 1997; Yao *et al*., 2003). In addition, AD is associated with other pathological processes, including failing mitochondrial function and oxidative stress (Bickford *et al*., 2000; Butterfield and Sultana, 2007; Perry *et al*., 2003; Wang *et al*., 2010), increased inflammatory response (Finch *et al*., 2002; Gemma *et al*., 2002; Ginsberg *et al*., 2006; Mrak and Griffin, 2001; Mucke *et al*., 2000; Rogers *et al*., 1996), protein misfolding (Forman *et al*., 2003; Stefani and Dobson, 2003), altered growth factor signaling (Mufson *et al*., 2007; Tuszynski and Gage, 1990; Williams *et al*., 2006), aberrant reentry of neurons into the cell cycle (Arendt *et al*., 2000; Bowser and Smith, 2002), lysosomal activation (Ginsberg *et al*., 2010; Nixon *et al*., 2001), endocrine alteration (Brinton, 2008; Landfield *et al*., 2007; Simpkins *et al*., 2005; Sohrabji and Lewis, 2006), insulin resistance (Craft, 2007; Gustafson, 2006; Whitmer *et al*., 2007; Yaffe *et al*., 2004), cholesterol dyshomeostasis (Petanceska *et al*., 2002; Puglielli *et al*., 2001), and calcium dysregulation. The latter plays an important role in normal brain aging as well as in some models of AD (Bezprozvanny and Mattson, 2008; Disterhoft *et al*., 1994; Foster and Norris, 1997; Gibson and Peterson, 1987; Khachaturian, 1989; Landfield, 1987; Michaelis *et al*., 1996; Nixon *et al*., 1994; Norris *et al*., 1998; Stutzmann, 2005; Stutzmann *et al*., 2007; Thibault *et al*., 2007; Wang *et al*., 2010), and may arise in part from a decrease in immunophilin-mediated stabilization of ryanodine receptors (Gant *et al*., 2011).

The complexity and number of changes associated with AD has impeded attempts to disentangle the processes important for pathogenesis or to define the roles of specific cell types in disease progression. Microarray analysis of the simultaneous expression of thousands of genes is well-suited to address complex processes and has been used effectively to provide overviews of the gene networks disturbed in AD (Colangelo *et al*., 2002; Ginsberg *et al*., 2006; Ginsberg *et al*., 2000; Liang *et al*., 2008; Loring *et al*., 2001; Pasinetti, 2001; Wang *et al*., 2010; Yao *et al*., 2003). Nevertheless, expression profiles vary substantially across cell types and regions (Bishop *et al*., 2010; Blalock *et al*., 2010; Burger, 2010; Ginsberg *et al*., 2006; Zahn *et al*., 2007; Zhao *et al*., 2001), and it is not yet clear how the expression signatures of specific cell/tissue types are related to early-stage AD.

In a prior study, we combined microarray technology with statistical correlation analyses to identify hippocampal gene expression changes associated with cognitive dysfunction and neurofibrillary tangles across a spectrum from incipient to severe AD (Blalock *et al*., 2004). Results of that study led us to propose that incipient AD was in part driven by aberrant activation of growth factors in oligodendrocytes and myelinated fiber tracts and, in turn, suppressive responses in other cell types (Blalock et al, 2004). However, because our study was conducted on hand-dissected frozen hippocampal CA1 blocks containing both white and gray matter, it was not possible to clearly distinguish their transcriptional changes. Further, when heterogeneous cell types/regions are mixed together, alterations in one component may oppose or dilute those in another, potentially obscuring important tissue-specific changes.

To overcome tissue heterogeneity problems, laser capture microdissection (LCM) technology and other techniques to isolate specific subregions and individual cell types have been employed in several AD studies (Ginsberg *et al*., 2010; Ginsberg *et al*., 2006; Liang *et al*., 2008). Here, we used a similar LCM approach to address some of the tissue-specific questions that were not clearly resolved in our prior study. In the present LCM study, we laser dissected formalin-fixed, paraffin-embedded (FFPE) sections from the same subjects (N = 30) analyzed in our earlier study (Blalock *et al*., 2004) and captured hippocampal CA1 gray matter (neuropil/neuronal somata) regions while largely excluding prominent white matter tracts (the perforant path, fimbria and alveus). Thus, this re-sampling of the same subjects provided a unique opportunity to directly compare results from similar samples containing or lacking significant white matter components, as well as to compare data from two disparate tissue fixation/collection approaches. If RNA integrity were generally comparable across these methods, we predicted many findings would correspond between the two studies, as both methods collected neuropil. However, we also hypothesized that, compared to our past analysis of white-matter-enriched hand-dissected CA1 tissue, the present analysis of white-matter-sparse tissue should detect fewer upregulated AD-associated genes, while also uncovering some previously obscured neuronal-specific genes/processes. The data reported here support these hypotheses, strengthening our model of white matter pathogenesis and revealing novel gray matter alterations with potential mechanistic and/or therapeutic implications.

2. Materials and Methods

2.1 Subjects, specimen preparation

Descriptions and categorization of the subjects were reported previously (Blalock et al, 2004). Brain sections from a total of 30 of the original 31 subjects were analyzed here. As in the prior study, we correlated gene expression with quantitative values on two AD marker scales (MiniMental Status Exam (MMSE) and neurofibrillary tangle (NFT) density), irrespective of clinical diagnosis. This strategy relied on quantitative markers to assess extent of disease progression rather than on categorization by clinico-pathologic criteria, which can be uncertain in borderline cases or when diagnostic markers disagree. However, for comparison and validation, the 30 subjects were also categorized into four categories of varying AD severity. Briefly, subjects (11 male, 19 female; average age 86.3 ± 1.4 years) were separated into four categories (control n = 8; incipient n = 7; moderate n = 8; severe n = 7) largely based on MMSE results (control- 27.6 ± 0.6; incipient- 24.3 ± 1.1; moderate- 16.5 ± 0.6; severe- 6.0 ± 1.4). For borderline cases, NFT count (control- 3.0 ± 1.1; incipient- 17.5 ± 8.2; moderate- 25.6 ± 3.5; severe- 32.7 ± 3.2) and Braak staging (control- 2.3 ± 0.4; incipient- 5.0 ± 0.5; moderate- 5.5 ± 0.2; severe- 5.8 ± 0.2) also informed categorization decisions.

For this study, formalin fixed, paraffin embedded (FFPE) specimens were used. Post mortem interval (PMI: 3.7 ± 0.6 hours); duration of direct formalin exposure (4.0 ± 1.2 days); and time in paraffin block (7.3 ± 0.2 years) did not differ significantly among groups ($p > 0.05$ in all tests; 1-ANOVA). Eight-μm sections from FFPE hippocampal blocks were mounted on PALM 1mm polyethylene naphthalate (PEN) membrane slides (Zeiss, Germany). Slides were de-waxed (2 × 10 min xylene, 2 × 10 min 100% EtOH, 1 × 10 min 90% EtOH, 1 × 10 min 70% EtOH, 1 × dH_20 5 min) and dehydrated (70% EtOH 10 min, 90 % EtOH 2 min, 2 × 100% EtOH 3 & 5 min, 2 × 100% xylene 5 & 10 min) to facilitate dissection and laser capture. Neuropathologists defined the CA1 region for each specimen using photomicrographs.

2.2 Laser Capture Microdissection

A Zeiss AxioObserver PALM Microbeam with RoboMover cap system was used to image, cut and capture specimens (Woods Hole, MA; courtesy of Zeiss- Fig. 1). The pathologist-identified CA1 region for each specimen (Fig. 1A) was used as a guide during laser capture. Specimen sections were targeted using a 5x cutting objective and were collected from regions of grossly defined gray matter (as defined in The Human Brain, Nolte, 2002) in hippocampal sub-field CA1, comprising the pyramidal cell layer and surrounding neuropil, largely excluding regions containing major white matter tracts (e.g., fimbria, alveus and perforant path) (Fig. 1B). Note that gray matter still contains astrocytes, capillaries, and other non-neuronal cells, as well as myelinated fibers (Vercellino *et al*., 2009), albeit considerably fewer of the latter than found in whole tissue dissections. The laser was set to cut through the PEN membrane to which the specimens were adhered, and then defocused and activated to capture (using the light pressure catapult) the cut regions of each sample. After each catapult, the capture area (siliconized eppendorf-style 0.5 ml centrifuge tube cap-one per slide) was visualized (Fig. 1B inset) to validate collection. On average, ~20 individual capture attempts were performed on each specimen and 1-2 capture attempts failed per sample. Captured material was stored dry at room temperature prior to RNA extraction and analysis.

2.3 RNA isolation and amplification

RNA was extracted using RecoverAll Total Nucleic Acid Isolation Kit for FFPE (Ambion) according to manufacturer's instructions (3h incubation at 55° C followed by glass fiber filtration). This system has recently been shown to outperform other FFPE methods/ kits regarding yield of amplifiable RNA (Okello *et al*., 2010). Quality assessment of extracted material was performed with the Paradise Reagent Quality Assessment Kit (Molecular Devices), as well as via NanoDrop (Thermoscientific). All samples yielded sufficient genetic material (>50 ng) for subsequent reactions. 50 ng of extracted purified nucleic acid underwent RNA amplification using WT-Ovation FFPE System (NuGen) followed by FL-Ovation cDNA Biotin Module V2 (NuGen) for labeling and microarray (Affymetrix HGU133 v2) hybridization. All 30 microarrays (one per each subject sample) performed within acceptable limits (Scaling factor: 32.6 +/− 3.7; RawQ: 1.28 +/− 0.01; GapDH 3′:5′: 1.48 +/− 0.08; % present 35.4 +/− 1.5) and were not significantly different across condition ($p < 0.5$ for all measures, 1-ANOVA). In comparison to prior work on frozen samples from the same subjects (Scaling factor: 5.9 +/− 0.6; RawQ 2.7 +/− 0.04; % present: 44.6 +/− 1.1), the increased scaling factor, decreased RawQ, and reduced % present all indicate reduced signal intensity, consistent with other reports of the dynamics of small FFPE sample extraction (Turner *et al*., 2011). Finally, the % present call, while lower than found in frozen tissue, is much greater than would be expected by chance (5%),suggesting that the extracted material contains substantial amounts of valid mRNA.

2.4 Microarray analysis and statistics

Probe sets were annotated, and transcriptional profiles were generated, using the MAS5 algorithm and annotation data sets (Affymetrix GCOS v. 1.1; HGU133 annotation October, 2003) in order to facilitate comparison with our prior work (Blalock *et al*., 2004). Raw data are available from the Gene Expression Omnibus (Barrett and Edgar, 2006) under accession ID GSE28146. Results were filtered for presence, redundancy, and annotation status and analyzed by Pearson's test for correlation with each subject's Mini-Mental Status Exam score and Neurofibrillary Tangle count. The false discovery rate (FDR) (Hochberg and Benjamini, 1990) was used to estimate the error of multiple testing's contribution to False Positives (see FDR, Fig 2). The DAVID suite of bioinformatic tools (Huang da *et al*., 2009), which identifies functional categories and biological processes/pathways that are statistically overrepresented by genes of interest, was used to identify processes/pathways from the Gene

Ontology (Ashburner *et al*., 2000) associated with the various lists of AD-correlated genes, using the 'table cluster' option. To reduce redundancy, only one representative pathway ($p \leq 0.05$; between 3 and 100 genes) from within each cluster is reported.

3. Results

3.1 Microarray analyses in laser captured samples

The comprehensive laser dissection data set was acquired from formalin-fixed, paraffin-embedded microscope slide specimens (from the same subjects as the original frozen tissue block study). Quality control results (Methods 2.3) showed that the laser dissection samples averaged 35% presence calls, ~7x the presence call rate that would be expected by chance (5%). Further, concordance at the presence call level among the 30 laser dissection arrays was also quite high. Genes rated present/absent on a single microarray tended to agree across all arrays (78.4% agreement).

Microarray signal intensities and presence calls were transferred to Excel and analyzed as in prior work (Blalock *et al*., 2004) (Fig. 2). Briefly, results were filtered to remove probe sets that were rated absent (< 4 presence calls across 30 chips) or poorly annotated (lacking or redundant gene symbol). The remaining 12,665 genes were correlated (Pearson's test) with MMSE scores as well as NFT counts across all subjects (Overall correlation). Genes with significant ($p \leq 0.05$) overall correlations were also sub-correlated with MMSE and NFT across only the control and incipient subjects (Incipient correlation).

3.1.1 AD-related genes—Results for all significantly correlated genes are provided as supplementary information (Supplemental Table 1). As seen in Fig. 2, correlation with MMSE appeared to explain a greater proportion of transcriptional profile variability than correlation with NFT, although there was a strong, statistically significant overlap between the two (747 genes; $p < 0.0001$, binomial test). However, 470/ 1566 (30%) of the NFT-correlated genes were also correlated across the incipient and control groups, whereas only 335/ 2646 (12.6%) of MMSE-correlated genes showed a similar incipient AD correlation. Hence, a greater proportion of NFT-correlated genes were associated with early disease progression, while cognitive measures appeared more strongly tied to later disease stages.

3.1.2 AD-related functional categories and pathways—Table 1 shows the functional processes found by DAVID analysis to be overrepresented by either downregulated or upregulated overall AD-correlated genes. Downregulated processes were strongly associated with neuronal function (synaptic components, ion channel activity, neurotransmitter receptors, axon, Ca2+ signaling) and, to a lesser extent, with energy production (glycolysis, mitochondrial components) and cell development (differentiation, transport, and filament structure). Conversely, upregulated categories included the now-stereotypical inflammatory (inflammatory response and complement activation) and iron homeostasis responses often associated with glial activation, as well as strong apoptotic signals. These patterns of downregulated neuronal and mitochondrial processes in conjunction with upregulated inflammatory and apoptotic pathways are highly similar to results reported in our prior work analyzing AD-associated microarray signatures from excised blocks of frozen hippocampal CA1 tissue (Blalock et al, 2004), as well to results from a number of studies by others (Wang *et al*., 2010). All significantly correlated genes in the present study are listed in Supplemental Table 1.

Nonetheless, some notable differences were found between processes identified in this study vs. those identified in our prior study. Among the most prominent was the present study's paucity, relative to the prior study, of upregulated genes related to growth, tumor suppression, transcription, chromatin remodeling, lipid metabolism, extracellular matrix,

cytoskeletal organization, oxidative stress, and some immune processes. For downregulated processes, the absence here of ubiquitin-dependent protein catabolic categories was particularly evident. Conversely, potentially important processes seen in laser dissected gray matter samples, including decreased regulation of Ca2+ release from ryanodine receptors, and increased vascular development, were not found in our prior work.

3.2 Direct comparisons with our prior study (Blalock et al, 2004)

The comprehensive analysis (section 3.1) of laser-dissected gray matter from the same subjects generally confirmed and extended many of our prior observations from frozen tissue blocks of CA1 material (Blalock *et al*., 2004). However, to more systematically test the degree of similarity between the two data sets (as well as to identify unique or missing signatures), we statistically compared the two studies as follows: The same probe level algorithm (MAS5) and annotation files were used for both the "laser dissection" and "tissue block" data. Further, testing for significant correlations was restricted to 10,475 probe sets that were perfect matches between the laser microdissection (Affymetrix HG U133 v.2) and tissue block (Affymetrix HG U133A) microarrays. At the presence call level, 59.4% (6,227/10,475) of probe sets were present in laser dissection, and 60.1% (6,338/ 10,475) were present in tissue block, with 5,065 present in both (~81% agreement). These results are highly unlikely by chance ($p < 0.0001$; binomial test), supporting the idea that detection sensitivities for the laser dissection and tissue block samples, at least at the presence call level prior to evaluation of AD-related gene signatures, were highly similar. Because presence in either study indicates a potential for correlation in at least one dataset, the list of common annotated genes available for testing correlations was expanded from 5,065 present in both studies to include genes present in at least one of the two studies, for a total of 7,537 testable genes.

All genes found to correlate overall with at least one AD marker (NFT or MMSE) were partitioned according to the data set in which they correlated ("tissue block", "laser dissection", or "both"; Fig. 3-Venn diagram) and the complete list of correlated genes is provided (Supplemental Table 2). Functional overrepresentation analysis (see Methods) was used to identify biological processes overrepresented by significant genes. The primary processes identified for each of the three Venn component gene lists are shown below (Tables 2-4).

3.2.1 Correlated with overall AD in both tissue block and laser captured samples—(Overlap in Venn diagram, Fig. 3 inset center; Table 2; Supplemental Table 2A). If the results from laser dissection samples are generally valid, then the laser dissection and tissue block data should have many significantly correlated genes in common. That is, the number of AD-correlated overlapping genes should be much higher than expected by chance. Further, that overlap should be relatively enriched in neuron-specific genes and relatively impoverished in white matter genes, compared with results that are unique to the tissue block analysis. As in prior work examining similarities among gene signatures (Blalock *et al*., 2010), we plotted the found:expected ratio for number of overlapping genes as a function of the p-value cutoff (α level) used to test for correlation in both datasets (Fig. 3). There was very strong agreement between the two data sets and at a p-value cutoff of 0.05, 509 genes, or more than 34x as many genes as would be expected by chance, were found in the overlap (Fig. 3 Venn diagram). This highly significant result ($p < 1.0\times10^{-16}$; binomial test) shows that the overlapping genomic signature is very unlikely to have been identified by chance. Of the 509 genes that exhibited correlation with overall AD in both studies (Supplemental Table 2A), nearly twice as many also exhibited correlation with incipient AD in the laser capture study (202 genes, ~40%) as in the tissue block study (110 genes, ~22%) ($p = 1.9\times10^{-14}$, binomial test), suggesting that laser captured gray matter

provided higher resolution and better signal-to-noise than mixed samples of gray and white matter.

Table 2 shows the functional processes found by DAVID analysis to be overrepresented by the 509 genes correlated with overall AD in both studies. It can be seen that these functional processes are generally similar to the processes identified in the comprehensive analysis of all genes in the laser capture study (Table 1).

3.2.2 Correlated with overall AD exclusively in tissue block samples—(Fig. 3 Venn diagram left; Table 3; Supplemental table 2B). The largest number of significantly correlated genes (1905, 1159 of which were upregulated), was found among those correlated exclusively within tissue block samples (Supplemental Table 2B). Finding more significant gene expression changes in tissue block specimens is perhaps not surprising, given that the blocks contained a more varied cell type population. In addition, the functional categories identified by DAVID analysis for these 1905 tissue block genes tended to have the strongest statistical significance (lowest p-values). The tissue block study's relative abundance of upregulated AD-associated genes is reflected statistically by a highly significant reduction ($p = 8.7\times10^{-6}$, binomial test) in the ratio of upregulated to downregulated AD-correlated genes in the laser dissection (1.26) vs. tissue block (1.46) studies (Fig. 3), indicating that many upregulated correlated genes were related to the white matter tracts included exclusively in those tissue block samples. Among downregulated categories, the 5 most significant (Table 3, left) appeared closely related to mitochondrial bioenergetics, while other downregulated categories were associated with axonal and synaptic activity. The upregulated AD gene signature in tissue block appeared heavily enriched with epigenetic and transcription factor-related processes (Table 3 right- chromosome organization, chromatin assembly, promoter binding, etc.).

3.2.3 Correlated with overall AD exclusively in laser dissection samples—(Fig. 3 Venn diagram right; Table 4; Supplemental table 2C). Downregulated genes that correlated with AD exclusively in laser dissected material were similar to those seen in both the comprehensive analysis (Table 1) as well as the overlapping region of the Venn diagram, suggesting that different genes from the same processes may be identified in the different analyses (see Discussion). Nonetheless, proportionately more downregulated genes identified exclusively in LCM gray matter samples represented processes associated with declining protein transport and processing, compared to those in the prior tissue block study. Among upregulated genes, the more than 500 that were associated with secretory, epigenetic, stress and transcription processes were correlated with AD at much weaker average significance levels than in the tissue block samples. However, LCM sample genes uniquely identified previously undetected alterations correlated with incipient AD, including upregulated vasculature development Table 4), as well as downregulation of genes important for stabilization of ryanodine receptor-related intracellular Ca2+ release (the latter in the comprehensive laser capture analysis, Table 1).

4. Discussion

The laser dissection protocol's gray matter-enriched collection technique appears to have facilitated identification of novel AD-associated processes, including downregulated stabilization of ryanodine-sensitive Ca2+ release and upregulated vasculature development. Although the laser microdissected region of CA1 is heavily vascularized (Marinkovic *et al*., 1992) and contains high densities of ryanodine receptors (Gant *et al*., 2011), these signals may have been diluted or masked by white matter expression patterns in the prior tissue block study. Accordingly, the appearance of novel processes in the present study confirms and extends results of others (Ginsberg *et al*., 2010; Ginsberg *et al*., 2006; Liang *et al*.,

2008) showing that laser dissection techniques can provide a higher resolution assessment of region-specific transcriptional profiles. Moreover, when contrasted with our prior data on hand-dissected CA1 that included white matter tracts, these selective gray matter analyses provide strong support for the view that the previously reported upregulated transcriptional, epigenetic, lipid transport, glial-immune and tumor suppressor responses in AD (Blalock *et al*., 2004), which were largely absent in the present study, are predominantly localized in and around the excluded white matter.

Comparison of the two studies also highlighted important technical issues. While there have been numerous investigations demonstrating that RNA extracted from FFPE tissue is suitable for quantitative assessment (Abdueva *et al*., 2010; Coudry *et al*., 2007; Farragher *et al*., 2008; Scicchitano *et al*., 2006; Turner *et al*., 2011), to our knowledge the present study is the first to make head-to-head comparisons of brain microarray data between FFPE tissue and frozen tissue blocks from the same human subjects. Apart from the apparent white-matter-related differences, there was substantial concordance between the two microarray studies, given that they were performed several years apart on samples collected and preserved very differently (laser dissected, formalin-fixed vs. hand dissected, frozen). Multiple gene networks altered in incipient AD and correlated with MMSE cognitive scores agreed closely across these studies, at both the gene and pathway levels (Overlap, Tables 2-4), particularly for downregulated neuronal processes.

Thus, this general concordance strongly indicates that the FFPE data are valid, and that the expression differences found between tissue block and laser dissection reflect, at least in part, differences in the cell types and sub-regions collected, rather than technical issues related to RNA integrity or extraction efficiency. Nonetheless, some non-specific procedural effects cannot be ruled out.

4.1 Similarities to other array studies

The conclusion that the FFPE material provides valid data is supported further by general agreement between the present LCM study and other gene expression analyses. One of the first studies of transcriptional profiles in AD selectively isolated tangle-bearing neurons (Ginsberg *et al*., 2000). Results showed significant reductions in genes associated with canonical AD neuropathology, including phosphatases/ kinases, glutamate and dopamine receptors, and cytoskeletal proteins, as well as upregulation of Cathepsin D. A subsequent study that surveyed multiple brain regions (Loring *et al*., 2001) found now-canonical upregulated inflammation, cell adhesion, cell proliferation and protein synthesis pathways in AD, as well as downregulated signal transduction, energy metabolism, stress response, synaptic vesicle synthesis/ function, calcium binding, and cytoskeletal pathways. An analysis of temporal gyrus found that downregulated synaptophysin directly correlated with, while downregulated alpha synapsin expression appeared to precede, AD-related changes (Pasinetti, 2001). Microarray analysis in the CA1 hippocampal subregion (Colangelo *et al*., 2002) found decreased transcription factor, neurotrophic factor, signaling, and synaptic activity along with increased inflammation in AD. A focused study of synapse-related gene expression changes in superior frontal gyrus (Yao *et al*., 2003) found downregulated dynamin 1 and syntaxin 1A expression. Studies of individually isolated brain neurons in AD have shown widespread downregulation of synaptic and cytoskeletal genes, as well as mitochondrial genes associated with reduced metabolism and altered expression of pathological hallmarks (Ginsberg *et al*., 2006; Liang *et al*., 2008). Moreover, a recent study in laser-dissected tangle-bearing neurons (Ginsberg *et al*., 2010) reported that Rab 5 and 7 upregulation correlated with cognitive decline during AD progression, supporting the hypothesis that increased endosomal activity, as reflected by Rab component upregulation, may enhance TrkB degradation and lead to neuronal dysfunction. Thus, among microarray studies of AD, there appears to be relatively good agreement across analyses, at least for

downregulated changes in neurons and gray matter and for upregulated inflammatory responses. However, the expression signatures of different regions/tissues/ cell types, and their selective vulnerability in AD remain relatively unexplored (reviewed in Wang *et al*., 2010).

4.2 Differences from previous studies in the functional processes identified here

As noted, some of the most prominent incipient AD-related changes in our earlier study (increases of growth-related and oncogenic transcription factors, chromatin modifiers, lipid regulators and tumor suppressors (Blalock *et al*., 2004) were largely absent in the laser dissection material (Tables 1, 2, and 3; Supplemental Table 2). This result is consistent with our model of incipient AD (Blalock *et al*., 2004) in which aberrant transcriptional processes in oligodendrocytes are proposed to trigger cascades that affect other cell types, providing a potential mechanistic explanation for the apparent progression of AD pathology along myelinated tracts. Of course, additional studies will be needed to further elucidate the role of white matter transcriptional changes in incipient AD.

Another notable difference from our previous study and studies of others is the detection here of novel changes in potentially important functional processes, including upregulation of vasculature development and downregulation of ryanodine receptor stabilization, both of which correlated strongly with incipient AD. These processes may well have important mechanistic implications. For example, Ca2+ dyshomeostasis has long been suspected of a role in brain aging and AD (see Introduction) and it was recently found that downregulation or disruption of the immunophilin FKBP1b (and possibly, FKBP1a) can destabilize and increase ryanodine receptor Ca2+ release in hippocampal neurons, creating an aging-like phenotype (Gant *et al*., 2011). Here, FKBP1a, two junctophilins and CALM 3, which also participate in ryanodine receptor stabilization, were found to be significantly downregulated and correlated with incipient AD (Supplemental Table 1), as was FKBP1b in the previous study (Blalock et al, 2004; their Table 3). Thus, further studies investigating the significance of ryanodine receptor destabilization in the progression of AD appear warranted by the present results.

Similarly, the upregulation of genes related to vasculature development also may have mechanistic implications. Although many, or most, of the 48 correlated genes populating this category (see Supplemental Table 3) have roles in development and growth of other tissue types, all have also been linked to vasculature development. While the functional significance of this is difficult to discern at present, it may be relevant that angiogenesis is a well-established co-factor in tumor growth, and plays a key role in retinal macular degeneration (Ambati, 2011).

A major challenge for future research on molecular pathogenesis of AD will be to determine how, or if, these novel gray matter changes interact with the putative white matter alterations or, for that matter, with any of the multiple other processes previously identified in our studies and studies of others. Clearly, some of the alterations found may be secondary or incidental correlates of AD. Nonetheless, multiple processes identified in our studies were correlated with incipient as well as with late-stage AD, and consequently appear at least to be candidates for primary processes.

4.3 Statistical issues

The overlap analysis (Fig. 3) reduces false positives, but does so at the cost of a likely increase in false negatives, in that a gene must meet the $p \leq 0.05$ criterion in two studies (Blalock *et al*., 2005). Therefore, the ‘true’ agreement between these two studies may be substantially greater than reported here. Nonetheless, the more than 34x increase in genes

agreeing between the two studies, compared to what should be expected by chance, illustrates that genes in the overlap analysis likely contain a very high proportion of true positive findings. It also should be noted that, because this approach assigns sets of genes to each exclusive Venn region based on a single p-value cutoff, genes attributed to one Venn region (Fig. 3, inset) may be borderline significant in another, effectively splitting a functional category across Venn regions. Upregulated immune activity, which appears in both the “overlap” and “tissue block” analyses may reflect this borderline effect.

5. Conclusions

Our results provide strong reciprocal validation for two technically dissimilar microarray analyses of Alzheimer’s disease. Gene expression values derived from laser dissected gray matter in formalin fixed, paraffin embedded specimens yielded a signature highly similar in many aspects to that measured in frozen tissue block specimens, including calcium regulation, synaptic, neuronal, inflammatory, and endosomal pathways- most of which have been identified in multiple studies (see section 4.1). Therefore, the discrepancies between the tissue block and laser dissection signatures did not appear to be due to random error, but to differences in the expression profiles of gray and white matter (the latter perhaps including the synaptic fields and glial processes immediately adjacent to myelinated tracts) . Although technical differences to some extent probably contribute to discordance between the two data sets, such effects appear minor and, further, it is highly unlikely that technical influences would exert themselves at the functional grouping level. That is, there is no *a priori* reason to expect that a particular functional category of genes would be more sensitive to formalin, laser dissection, or amplification protocols- these effects should seemingly distribute randomly, or at least, not partition discreetly within biological pathways. Thus, we conclude that the targeted difference in tissue components is the most likely and most parsimonious explanation for many of those aspects of the transcriptional profile that differed between our two studies.

Supplementary Material

Refer to Web version on PubMed Central for supplementary material.

Acknowledgments

We thank Sonya Anderson and Ela Patel from the Sanders-Brown Center on Aging for sectioning and mounting hippocampal specimens, Jeff Gilbert and Zeiss Microscopy, as well as Woods Hole Research Center for generously allowing us to use their Zeiss PALM Microbeam system, Anjali Chhabra for performing RNA isolation and amplification protocols, and Dr. Kuey Chu Chen and Donna Wall of the University of Kentucky Microarray Core Facility for microarray hybridization and scanning. This work was supported in part by grants from the University of Kentucky Alzheimer’s Disease Center (AG028383) and the NIH Research Resources Center (S10RR024704) (to E.M.B.), and by grants AG034605, AG004542 and P01AG010836 from the National Institute on Aging (to P.W.L.).

References

Abdueva D, Wing M, Schaub B, Triche T, Davicioni E. Quantitative expression profiling in formalin-fixed paraffin-embedded samples by affymetrix microarrays. J Mol Diagn. 2010; 12:409–417. [PubMed: 20522636]

Ambati J. Age-related macular degeneration and the other double helix. The Cogan Lecture. Investigative ophthalmology & visual science. 2011; 52:2165–2169. [PubMed: 21471430]

Arendt T, Holzer M, Stobe A, Gartner U, Luth HJ, Bruckner MK, Ueberham U. Activated mitogenic signaling induces a process of dedifferentiation in Alzheimer’s disease that eventually results in cell death. Ann N Y Acad Sci. 2000; 920:249–255. [PubMed: 11193159]

Ashburner M, Ball CA, Blake JA, Botstein D, Butler H, Cherry JM, Davis AP, Dolinski K, Dwight SS, Eppig JT, Harris MA, Hill DP, Issel-Tarver L, Kasarskis A, Lewis S, Matese JC, Richardson JE, Ringwald M, Rubin GM, Sherlock G. Gene ontology: tool for the unification of biology. The Gene Ontology Consortium. Nat Genet. 2000; 25:25–29. [PubMed: 10802651]

Barrett T, Edgar R. Gene expression omnibus: microarray data storage, submission, retrieval, and analysis. Methods Enzymol. 2006; 411:352–369. [PubMed: 16939800]

Bezprozvanny I, Mattson MP. Neuronal calcium mishandling and the pathogenesis of Alzheimer's disease. Trends Neurosci. 2008; 31:454–463. [PubMed: 18675468]

Bickford PC, Gould T, Briederick L, Chadman K, Pollock A, Young D, Shukitt-Hale B, Joseph J. Antioxidant-rich diets improve cerebellar physiology and motor learning in aged rats. Brain Res. 2000; 866:211–217. [PubMed: 10825496]

Bishop NA, Lu T, Yankner BA. Neural mechanisms of ageing and cognitive decline. Nature. 2010; 464:529–535. [PubMed: 20336135]

Blalock EM, Chen KC, Stromberg AJ, Norris CM, Kadish I, Kraner SD, Porter NM, Landfield PW. Harnessing the power of gene microarrays for the study of brain aging and Alzheimer's disease: statistical reliability and functional correlation. Ageing Res Rev. 2005; 4:481–512. [PubMed: 16257272]

Blalock EM, Geddes JW, Chen KC, Porter NM, Markesbery WR, Landfield PW. Incipient Alzheimer's disease: microarray correlation analyses reveal major transcriptional and tumor suppressor responses. Proc Natl Acad Sci U S A. 2004; 101:2173–2178. [PubMed: 14769913]

Blalock EM, Grondin R, Chen KC, Thibault O, Thibault V, Pandya JD, Dowling A, Zhang Z, Sullivan P, Porter NM, Landfield PW. Aging-related gene expression in hippocampus proper compared with dentate gyrus is selectively associated with metabolic syndrome variables in rhesus monkeys. J Neurosci. 2010; 30:6058–6071. [PubMed: 20427664]

Bowser R, Smith MA. Cell cycle proteins in Alzheimer's disease: plenty of wheels but no cycle. J Alzheimers Dis. 2002; 4:249–254. [PubMed: 12226545]

Brinton RD. Estrogen regulation of glucose metabolism and mitochondrial function: therapeutic implications for prevention of Alzheimer's disease. Adv Drug Deliv Rev. 2008; 60:1504–1511. [PubMed: 18647624]

Burger C. Region-specific genetic alterations in the aging hippocampus: implications for cognitive aging. Front Aging Neurosci. 2010; 2:140. [PubMed: 21048902]

Butterfield DA, Sultana R. Redox proteomics identification of oxidatively modified brain proteins in Alzheimer's disease and mild cognitive impairment: insights into the progression of this dementing disorder. Journal of Alzheimer's disease : JAD. 2007; 12:61–72. [PubMed: 17851195]

Colangelo V, Schurr J, Ball MJ, Pelaez RP, Bazan NG, Lukiw WJ. Gene expression profiling of 12633 genes in Alzheimer hippocampal CA1: transcription and neurotrophic factor down-regulation and up-regulation of apoptotic and pro-inflammatory signaling. J Neurosci Res. 2002; 70:462–473. [PubMed: 12391607]

Coudry RA, Meireles SI, Stoyanova R, Cooper HS, Carpino A, Wang X, Engstrom PF, Clapper ML. Successful application of microarray technology to microdissected formalin-fixed, paraffin-embedded tissue. J Mol Diagn. 2007; 9:70–79. [PubMed: 17251338]

Craft S. Insulin resistance and Alzheimer's disease pathogenesis: potential mechanisms and implications for treatment. Current Alzheimer research. 2007; 4:147–152. [PubMed: 17430239]

Davies P, Koppel J. Mechanism-based treatments for Alzheimer's disease. Dialogues Clin Neurosci. 2009; 11:159–169. [PubMed: 19585951]

Disterhoft JF, Moyer JR Jr. Thompson LT. The calcium rationale in aging and Alzheimer's disease. Evidence from an animal model of normal aging. Ann N Y Acad Sci. 1994; 747:382–406. [PubMed: 7847686]

Farragher SM, Tanney A, Kennedy RD, Harkin D. Paul. RNA expression analysis from formalin fixed paraffin embedded tissues. Histochem Cell Biol. 2008; 130:435–445. [PubMed: 18679706]

Finch, CE.; Morgan, T.; Rozovsky, I.; Xie, Z.; Weindruch, R.; Prolla, T. Microglia and aging in the brain. In: WJ, S., editor. Microglia in the Degenerating and Regenerating CNS. Springer-Verlag; New York: 2002.

Forman MS, Lee VM, Trojanowski JQ. 'Unfolding' pathways in neurodegenerative disease. Trends Neurosci. 2003; 26:407–410. [PubMed: 12900170]

Foster TC, Norris CM. Age-associated changes in Ca(2+)-dependent processes: relation to hippocampal synaptic plasticity. Hippocampus. 1997; 7:602–612. [PubMed: 9443057]

Gant JC, Chen KC, Norris CM, Kadish I, Thibault O, Blalock EM, Porter NM, Landfield PW. Disrupting function of FK506-binding protein 1b/12.6 induces the Ca(2)+-dysregulation aging phenotype in hippocampal neurons. J Neurosci. 2011; 31:1693–1703. [PubMed: 21289178]

Gemma C, Mesches MH, Sepesi B, Choo K, Holmes DB, Bickford PC. Diets enriched in foods with high antioxidant activity reverse age-induced decreases in cerebellar beta-adrenergic function and increases in proinflammatory cytokines. J Neurosci. 2002; 22:6114–6120. [PubMed: 12122072]

Gibson GE, Peterson C. Calcium and the aging nervous system. Neurobiol Aging. 1987; 8:329–343. [PubMed: 3306433]

Ginsberg SD, Alldred MJ, Counts SE, Cataldo AM, Neve RL, Jiang Y, Wuu J, Chao MV, Mufson EJ, Nixon RA, Che S. Microarray analysis of hippocampal CA1 neurons implicates early endosomal dysfunction during Alzheimer's disease progression. Biol Psychiatry. 2010; 68:885–893. [PubMed: 20655510]

Ginsberg SD, Che S, Counts SE, Mufson EJ. Single cell gene expression profiling in Alzheimer's disease. NeuroRx. 2006; 3:302–318. [PubMed: 16815214]

Ginsberg SD, Hemby SE, Lee VM, Eberwine JH, Trojanowski JQ. Expression profile of transcripts in Alzheimer's disease tangle-bearing CA1 neurons. Ann Neurol. 2000; 48:77–87. [PubMed: 10894219]

Gustafson D. Adiposity indices and dementia. Lancet Neurol. 2006; 5:713–720. [PubMed: 16857578]

Hardy J, Selkoe DJ. The amyloid hypothesis of Alzheimer's disease: progress and problems on the road to therapeutics. Science. 2002; 297:353–356. [PubMed: 12130773]

Hochberg Y, Benjamini Y. More powerful procedures for multiple significance testing. Stat Med. 1990; 9:811–818. [PubMed: 2218183]

Huang da W, Sherman BT, Lempicki RA. Systematic and integrative analysis of large gene lists using DAVID bioinformatics resources. Nat Protoc. 2009; 4:44–57. [PubMed: 19131956]

Johnson GV, Bailey CD. Tau, where are we now? J Alzheimers Dis. 2002; 4:375–398. [PubMed: 12446970]

Khachaturian ZS. The role of calcium regulation in brain aging: reexamination of a hypothesis. Aging (Milano). 1989; 1:17–34. [PubMed: 2488296]

Klein WL, Krafft GA, Finch CE. Targeting small Abeta oligomers: the solution to an Alzheimer's disease conundrum? Trends Neurosci. 2001; 24:219–224. [PubMed: 11250006]

Landfield PW. 'Increased calcium-current' hypothesis of brain aging. Neurobiol Aging. 1987; 8:346–347. [PubMed: 3627350]

Landfield PW, Blalock EM, Chen KC, Porter NM. A new glucocorticoid hypothesis of brain aging: implications for Alzheimer's disease. Curr Alzheimer Res. 2007; 4:205–212. [PubMed: 17430248]

Liang WS, Dunckley T, Beach TG, Grover A, Mastroeni D, Ramsey K, Caselli RJ, Kukull WA, McKeel D, Morris JC, Hulette CM, Schmechel D, Reiman EM, Rogers J, Stephan DA. Altered neuronal gene expression in brain regions differentially affected by Alzheimer's disease: a reference data set. Physiol Genomics. 2008; 33:240–256. [PubMed: 18270320]

Loring JF, Wen X, Lee JM, Seilhamer J, Somogyi R. A gene expression profile of Alzheimer's disease. DNA Cell Biol. 2001; 20:683–695. [PubMed: 11788046]

Marinkovic S, Milisavljevic M, Puskas L. Microvascular anatomy of the hippocampal formation. Surg Neurol. 1992; 37:339–349. [PubMed: 1631758]

Masliah E, Mallory M, Hansen L, DeTeresa R, Alford M, Terry R. Synaptic and neuritic alterations during the progression of Alzheimer's disease. Neurosci Lett. 1994; 174:67–72. [PubMed: 7970158]

Michaelis ML, Bigelow DJ, Schoneich C, Williams TD, Ramonda L, Yin D, Huhmer AF, Yao Y, Gao J, Squier TC. Decreased plasma membrane calcium transport activity in aging brain. Life sciences. 1996; 59:405–412. [PubMed: 8761328]

Morgan D. Learning and memory deficits in APP transgenic mouse models of amyloid deposition. Neurochem Res. 2003; 28:1029–1034. [PubMed: 12737527]

Morris M, Maeda S, Vossel K, Mucke L. The many faces of tau. Neuron. 2011; 70:410–426. [PubMed: 21555069]

Mrak RE, Griffin WS. Interleukin-1, neuroinflammation, and Alzheimer's disease. Neurobiol Aging. 2001; 22:903–908. [PubMed: 11754997]

Mucke L, Masliah E, Yu GQ, Mallory M, Rockenstein EM, Tatsuno G, Hu K, Kholodenko D, Johnson-Wood K, McConlogue L. High-level neuronal expression of abeta 1-42 in wild-type human amyloid protein precursor transgenic mice: synaptotoxicity without plaque formation. J Neurosci. 2000; 20:4050–4058. [PubMed: 10818140]

Mufson EJ, Counts SE, Fahnestock M, Ginsberg SD. Cholinotrophic molecular substrates of mild cognitive impairment in the elderly. Current Alzheimer research. 2007; 4:340–350. [PubMed: 17908035]

Mullan M, Crawford F. The molecular genetics of Alzheimer's disease. Mol Neurobiol. 1994; 9:15–22. [PubMed: 7888092]

Nixon RA, Mathews PM, Cataldo AM. The neuronal endosomal-lysosomal system in Alzheimer's disease. J Alzheimers Dis. 2001; 3:97–107. [PubMed: 12214078]

Nixon RA, Saito KI, Grynspan F, Griffin WR, Katayama S, Honda T, Mohan PS, Shea TB, Beermann M. Calcium-activated neutral proteinase (calpain) system in aging and Alzheimer's disease. Ann N Y Acad Sci. 1994; 747:77–91. [PubMed: 7847693]

Noble W, Olm V, Takata K, Casey E, Mary O, Meyerson J, Gaynor K, LaFrancois J, Wang L, Kondo T, Davies P, Burns M, Veeranna, Nixon R, Dickson D, Matsuoka Y, Ahlijanian M, Lau LF, Duff K. Cdk5 is a key factor in tau aggregation and tangle formation in vivo. Neuron. 2003; 38:555–565. [PubMed: 12765608]

Norris CM, Halpain S, Foster TC. Reversal of age-related alterations in synaptic plasticity by blockade of L-type Ca2+ channels. J Neurosci. 1998; 18:3171–3179. [PubMed: 9547225]

Okello JB, Zurek J, Devault AM, Kuch M, Okwi AL, Sewankambo NK, Bimenya GS, Poinar D, Poinar HN. Comparison of methods in the recovery of nucleic acids from archival formalin-fixed paraffin-embedded autopsy tissues. Anal Biochem. 2010; 400:110–117. [PubMed: 20079706]

Pasinetti GM. Use of cDNA microarray in the search for molecular markers involved in the onset of Alzheimer's disease dementia. J Neurosci Res. 2001; 65:471–476. [PubMed: 11550214]

Perry G, Nunomura A, Raina AK, Aliev G, Siedlak SL, Harris PL, Casadesus G, Petersen RB, Bligh-Glover W, Balraj E, Petot GJ, Smith MA. A metabolic basis for Alzheimer disease. Neurochemical research. 2003; 28:1549–1552. [PubMed: 14570400]

Petanceska SS, DeRosa S, Olm V, Diaz N, Sharma A, Thomas-Bryant T, Duff K, Pappolla M, Refolo LM. Statin therapy for Alzheimer's disease: will it work? J Mol Neurosci. 2002; 19:155–161. [PubMed: 12212773]

Price DL, Sisodia SS. Mutant genes in familial Alzheimer's disease and transgenic models. Annu Rev Neurosci. 1998; 21:479–505. [PubMed: 9530504]

Puglielli L, Konopka G, Pack-Chung E, Ingano LA, Berezovska O, Hyman BT, Chang TY, Tanzi RE, Kovacs DM. Acyl-coenzyme A: cholesterol acyltransferase modulates the generation of the amyloid beta-peptide. Nat Cell Biol. 2001; 3:905–912. [PubMed: 11584272]

Rogers J, Webster S, Lue LF, Brachova L, Civin WH, Emmerling M, Shivers B, Walker D, McGeer P. Inflammation and Alzheimer's disease pathogenesis. Neurobiol Aging. 1996; 17:681–686. [PubMed: 8892340]

Scheff SW, Price DA. Alzheimer's disease-related synapse loss in the cingulate cortex. J Alzheimers Dis. 2001; 3:495–505. [PubMed: 12214036]

Scicchitano MS, Dalmas DA, Bertiaux MA, Anderson SM, Turner LR, Thomas RA, Mirable R, Boyce RW. Preliminary comparison of quantity, quality, and microarray performance of RNA extracted from formalin-fixed, paraffin-embedded, and unfixed frozen tissue samples. J Histochem Cytochem. 2006; 54:1229–1237. [PubMed: 16864893]

Simpkins JW, Wen Y, Perez E, Yang S, Wang X. Role of nonfeminizing estrogens in brain protection from cerebral ischemia: an animal model of Alzheimer's disease neuropathology. Annals of the New York Academy of Sciences. 2005; 1052:233–242. [PubMed: 16024766]

Sohrabji F, Lewis DK. Estrogen-BDNF interactions: implications for neurodegenerative diseases. Front Neuroendocrinol. 2006; 27:404–414. [PubMed: 17069877]

Stefani M, Dobson CM. Protein aggregation and aggregate toxicity: new insights into protein folding, misfolding diseases and biological evolution. J Mol Med. 2003; 81:678–699. [PubMed: 12942175]

Stutzmann GE. Calcium dysregulation, IP3 signaling, and Alzheimer's disease. Neuroscientist. 2005; 11:110–115. [PubMed: 15746379]

Stutzmann GE, Smith I, Caccamo A, Oddo S, Parker I, Laferla F. Enhanced ryanodine-mediated calcium release in mutant PS1-expressing Alzheimer's mouse models. Ann N Y Acad Sci. 2007; 1097:265–277. [PubMed: 17413028]

Sze CI, Troncoso JC, Kawas C, Mouton P, Price DL, Martin LJ. Loss of the presynaptic vesicle protein synaptophysin in hippocampus correlates with cognitive decline in Alzheimer disease. J Neuropathol Exp Neurol. 1997; 56:933–944. [PubMed: 9258263]

Tanzi RE, Bertram L. New frontiers in Alzheimer's disease genetics. Neuron. 2001; 32:181–184. [PubMed: 11683989]

Thibault O, Gant JC, Landfield PW. Expansion of the calcium hypothesis of brain aging and Alzheimer's disease: minding the store. Aging Cell. 2007; 6:307–317. [PubMed: 17465978]

Turner L, Heath JD, Kurn N. Gene expression profiling of RNA extracted from FFPE tissues: NuGEN technologies' whole-transcriptome amplification system. Methods Mol Biol. 2011; 724:269–280. [PubMed: 21370019]

Tuszynski MH, Gage FH. Potential use of neurotrophic agents in the treatment of neurodegenerative disorders. Acta Neurobiol Exp (Wars). 1990; 50:311–322. [PubMed: 2130651]

Vercellino M, Masera S, Lorenzatti M, Condello C, Merola A, Mattioda A, Tribolo A, Capello E, Mancardi GL, Mutani R, Giordana MT, Cavalla P. Demyelination, inflammation, and neurodegeneration in multiple sclerosis deep gray matter. Journal of neuropathology and experimental neurology. 2009; 68:489–502. [PubMed: 19525897]

Wang X, Michaelis ML, Michaelis EK. Functional genomics of brain aging and Alzheimer's disease: focus on selective neuronal vulnerability. Curr Genomics. 2010; 11:618–633. [PubMed: 21629439]

Whitmer RA, Gunderson EP, Quesenberry CP Jr. Zhou J, Yaffe K. Body mass index in midlife and risk of Alzheimer disease and vascular dementia. Current Alzheimer research. 2007; 4:103–109. [PubMed: 17430231]

Williams BJ, Eriksdotter-Jonhagen M, Granholm AC. Nerve growth factor in treatment and pathogenesis of Alzheimer's disease. Prog Neurobiol. 2006; 80:114–128. [PubMed: 17084014]

Yaffe K, Blackwell T, Kanaya AM, Davidowitz N, Barrett-Connor E, Krueger K. Diabetes, impaired fasting glucose, and development of cognitive impairment in older women. Neurology. 2004; 63:658–663. [PubMed: 15326238]

Yao PJ, Zhu M, Pyun EI, Brooks AI, Therianos S, Meyers VE, Coleman PD. Defects in expression of genes related to synaptic vesicle trafficking in frontal cortex of Alzheimer's disease. Neurobiol Dis. 2003; 12:97–109. [PubMed: 12667465]

Zahn JM, Poosala S, Owen AB, Ingram DK, Lustig A, Carter A, Weeraratna AT, Taub DD, Gorospe M, Mazan-Mamczarz K, Lakatta EG, Boheler KR, Xu X, Mattson MP, Falco G, Ko MS, Schlessinger D, Firman J, Kummerfeld SK, Wood WH 3rd, Zonderman AB, Kim SK, Becker KG. AGEMAP: a gene expression database for aging in mice. PLoS Genet. 2007; 3:e201. [PubMed: 18081424]

Zhao X, Lein ES, He A, Smith SC, Aston C, Gage FH. Transcriptional profiling reveals strict boundaries between hippocampal subregions. J Comp Neurol. 2001; 441:187–196. [PubMed: 11745644]

Research Highlights

- Subjects (N=30) spanned control, incipient, moderate and severe Alzheimer's disease
- Focused on microarray analyses of laser-dissected hippocampal gray matter
- Array profiles largely agreed with a prior study of combined white and gray matter
- Unique gray-matter AD changes included ryanodine and vascular pathways
- Unique white-matter AD changes included epigenetic and transcriptional pathways

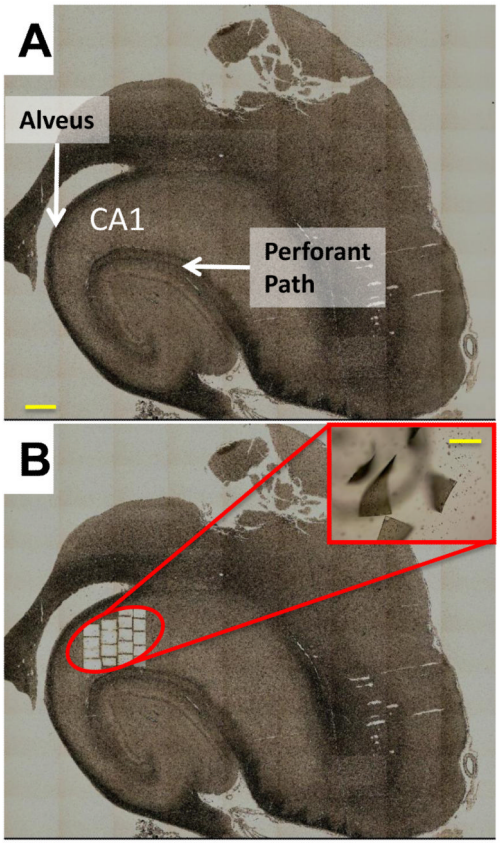

Figure 1. Representative images of laser capture process

A. Reconstructed image of human hippocampal section of CA1 region before laser cut and capture process. Associated white matter tracts, which appear as dark bundles, are labeled (alveus, perforant path). *Calibration bar* (yellow) = 1 mm. **B.** Same section after cut and capture process. Note that sampling region largely excludes white matter tracts. *Inset:* Laser pressure micro-catapulted sections in the capture region. *Calibration bar* (yellow) = 300 μm.

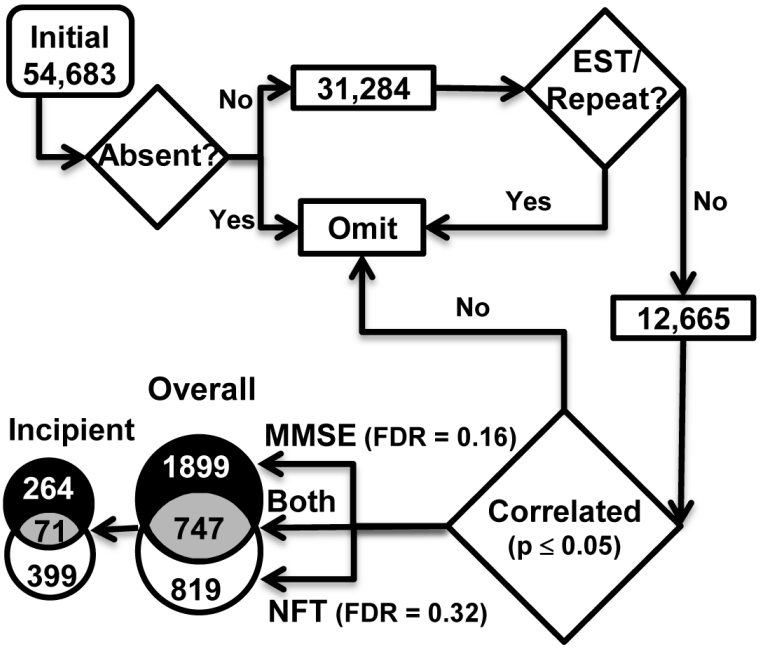

Figure 2. Flowchart of microarray correlation analysis procedure

Pre-statistical filtering omitted probe sets with poor annotation and/or low quality signal. Each of the remaining genes was correlated (Pearson's test) with MMSE scores and NFT counts across all 30 subjects (Overall correlation). If genes were found to correlate significantly with either marker overall, then a *post-hoc* correlation test across the subset of 15 subjects in the control and incipient groups (incipient correlation) was also performed. Numbers of significant genes were separated based on the AD marker (MMSE or NFT, or both) with which they were correlated. All genes significant in MMSE and/or NFT were used for subsequent functional overrepresentation analysis (Table 1).

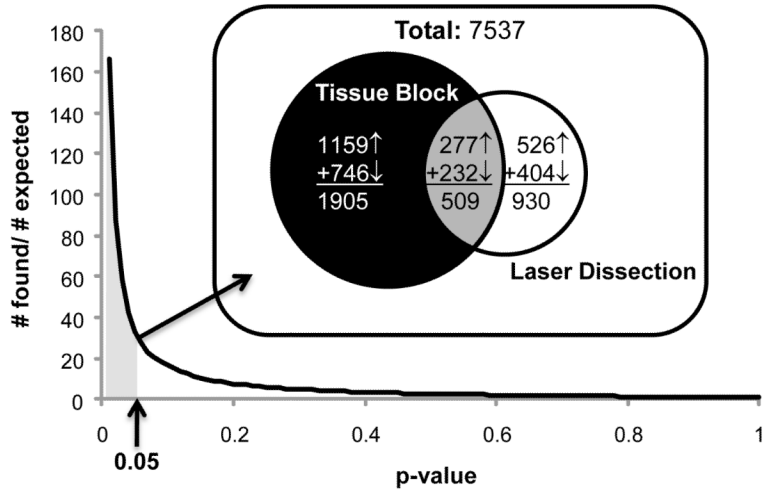

Figure 3. Comparing tissue block and laser capture dissection gene signatures

The two studies were conducted six years apart using different microarray platforms. For the 7537 gene probes that were present and annotated in both studies, the number of genes that showed correlations with an AD marker in both the tissue block and laser dissection samples (overlap) was determined. At extremely high (relaxed) p-value criteria for correlation significance (right), all genes are expected by chance to correlate with AD in both studies and all genes were found in the overlap (found:expected = 1.0). As p-value criterion stringency increases toward the left, the number of genes expected to correlate significantly in both studies by chance alone falls precipitously, as would the number actually found if there were little true overlap (maintaining a ratio of ~ 1.0). However, with increasing p-value stringency the found:expected ratio rises sharply, particularly at p-values below 0.05, indicating that far more genes were found to agree between studies than would be expected by chance. *Inset*- Venn Diagram: Using the 0.05 cutoff (gray shaded area, arrow), ~34 times as many overlapping genes as expected by chance was identified. Functional overrepresentation analysis was performed for genes encompassed within each region of the Venn diagram (section 3.2).

Table 1

Functional categories/ processes overrepresented by AD-correlated genes identified in laser-captured hippocampal gray matter.

Categories/ processes shown are those significantly overrepresented ($p \leq 0.05$) by genes correlated with AD markers in the overall AD and the incipient AD analyses. Categories are separated by direction of change and sorted by p-value. To reduce redundancy, only one representative functional category from each identified cluster of functions was selected. Processes not identified in the previous tissue block study include regulation of ryanodine-sensitive Ca2+ release and vasculature development. Column headings: Overall: results from genes significant in the overall correlation analysis; Incipient: results from genes also significant in the incipient correlation analysis; #: Number of genes significant; P- val: probability of overrepresentation; modified Fisher's exact test p-value provided by DAVID bioinformatic analysis software. Supplemental Table 1 lists all significant genes.

	Overall		Incipient	
Downregulated with AD	**#**	**P- val**	**#**	**P- val**
synapse	73	1.25×10^{-10}	17	0.0005
synaptic transmission	59	7.23×10^{-09}	12	0.0171
extracellular ligand-gated ion channel activity	15	2.77×10^{-05}	04	0.0469
axon	33	2.97×10^{-05}	09	0.0070
synaptic vesicle	19	9.55×10^{-05}	06	0.0090
ion transmembrane transporter activity	84	1.22×10^{-04}	18	0.0348
regulation of neuron differentiation	26	3.35×10^{-04}	09	0.0026
cation-transporting ATPase activity	12	4.09×10^{-04}	04	0.0298
glycolysis	12	6.89×10^{-04}	04	0.0372
clathrin-coated vesicle	24	0.0030	08	0.0084
regulation of transport	47	0.0038	12	0.0395
mitochondrial part	76	0.0113	18	0.0364
GABA-A receptor activity	06	0.0263	03	0.0443
*regulation of ryanodine-sensitive calcium-release channel activity	04	0.0414	03	0.0106
intermediate filament organization	04	0.0414	03	0.0106
mitochondrial membrane part	20	0.0419	08	0.0079
Upregulated with AD				
*vasculature development	48	2.62×10^{-06}	14	0.0165
negative regulation of developmental process	46	8.26×10^{-06}	14	0.0140
positive regulation of programmed cell death	68	2.11×10^{-04}	22	0.0103
serine-type endopeptidase inhibitor activity	14	0.0049	06	0.0232
inflammatory response	37	0.0060	14	0.0140
iron ion homeostasis	09	0.0091	05	0.0105
complement activation	08	0.0114	04	0.0363
apoptosis	80	0.0140	29	0.0071
induction of apoptosis by extracellular signals	22	0.0142	10	0.0088
actin cytoskeleton organization	37	0.0148	13	0.0448
response to vitamin	13	0.0207	06	0.0310

(*) categories unique to laser dissected material.

Table 2

Functional categories overrepresented by genes correlated with AD markers in both studies (Venn diagram overlap-Supplemental Table 2A).

Functional categories/ processes significantly ($p \leq 0.05$) downregulated (left) or upregulated (right) and correlated with overall AD in both laser-dissected and tissue block samples. The # genes significant as well as probability of overrepresentation (P-val) are given.

Downregulated	#	P -val	Upregulated	#	P -val
neuron projection	24	5.55×10^{-7}	kinase activity	31	0.004
precursor metabolites and energy	23	1.00×10^{-6}	transcription repressor	16	0.006
transmission of nerve impulse	23	1.36×10^{-6}	negative reg. differentiation	12	0.006
transporter activity	39	5.67×10^{-6}	complement activation	05	0.007
synapse part	18	6.60×10^{-6}	regulation of proliferation	30	0.009
neuron differentiation	21	5.54×10^{-5}	extracellular matrix	13	0.009
glycolysis	07	1.20×10^{-4}	inflammatory response	14	0.014
cellular ion homeostasis	17	0.001	transcr. RNA pol II promoter	26	0.017
intermediate filament assembly	03	0.003	mitotic interphase	08	0.027
cytoplasmic vesicle	21	0.006	microtub. organizing center	10	0.027
cognition	17	0.006	calmodulin binding	08	0.049
cellular macromolecule localization	18	0.008			
regulation of hormone levels	08	0.008			
microtubule associated complex	07	0.009			
apoptosis cell structure disassembly	04	0.009			
regulation of neuron differentiation	08	0.009			
cellular respiration	08	0.009			
unfolded protein binding	08	0.013			
voltage-gated channel activity	08	0.016			
calcium ion binding	22	0.019			
protein oligomerization	09	0.029			
extracell.glutamate-gated ion channel	03	0.037			

Table 3

Functional categories overrepresented by genes uniquely correlated with AD in tissue block samples (Venn diagram, left-Supplemental Table 2B).

Significant downregulated (left) and upregulated (right) biological processes ($p \leq 0.05$) overrepresented by correlated genes found exclusively in tissue block. Note the high proportion of processes associated with transcription, chromatin modification, immune functions, oxidative stress and lipid handling among upregulated categories (right). # genes significant as well as probability of overrepresentation (P-val) are given.

Downregulated	#	P -val	Upregulated	#	P -val
precursor metabolites and energy	62	1.38×10^{-14}	chromosome organization	67	2.63×10^{-05}
cellular respiration	32	1.05×10^{-12}	chromatin assembly or disassembly	21	9.23×10^{-04}
H+transmembrane transporter activity	28	1.84×10^{-12}	promoter binding	15	0.0025
mitochondrial matrix	40	6.00×10^{-08}	transcription activator activity	57	0.0031
aerobic respiration	13	2.91×10^{-05}	extracellular matrix	37	0.0038
glutamate catabolic process	05	0.0012	T cell activation	22	0.0047
transporter activity	81	0.0014	histone acetyltransferase complex	12	0.0061
cation-transporting ATPase activity	10	0.0017	positive regulation of lipid storage	05	0.0066
phosphorylation	70	0.0021	immune system development	36	0.0088
transmission of nerve impulse	36	0.0037	intracellular induction of apoptosis	13	0.0099
glutamate metabolic process	06	0.0042	regulation of transcription factor activity	19	0.0115
+reg. ubiquitin-protein ligase activity	14	0.0044	regulation of immune response	28	0.0173
ubiquitin-dependent catabolic process	27	0.0047	regulation of ARF GTPase activity	08	0.0193
nervous system development	83	0.0053	nuclear chromatin	12	0.0288
synaptic vesicle membrane	07	0.0069	histone deacetylase activity	05	0.0378
ubiquitin thiolesterase activity	10	0.0082	interphase of mitotic cell cycle	19	0.0397
nucleoside diphosphate metabolic process	05	0.0124	transcription repressor activity	41	0.0405
mitochondrial ribosome	08	0.0158	cellular response to oxidative stress	10	0.0408
response to glucose stimulus	08	0.0207	regulation of lipid transport	07	0.0481
regulation of translational initiation	08	0.0207			
microtubule associated complex	12	0.0234			
peptidase activity	35	0.0268			
exocytosis	13	0.0330			
translation	31	0.0380			

Table 4

Functional categories overrepresented by genes correlated with overall AD uniquely in laser-dissected samples (Venn diagram, left- Supplemental Table 2C).

Significant downregulated (left) and upregulated (right) biological categories/ processes overrepresented ($p \leq 0.05$) by AD-correlated genes found exclusively in laser-dissected samples. Note novel blood vessel development category (right). # genes significant as well as probability (P-val) are given.

Downregulated	#	P -val	Upregulated	#	P -val
protein transport	40	0.0050	blood vessel development	22	0.0011
ion channel activity	19	0.0062	tube morphogenesis	13	0.0013
transporter activity	46	0.0069	release of cyt. c from mitochondria	06	0.0029
N-methyltransferase activity	06	0.0083	regulation of protein kinase cascade	22	0.0037
chloride channel activity	07	0.0105	secretory granule	15	0.0066
heat shock protein binding	08	0.0113	extracellular structure organization	14	0.0136
glucose metabolic process	12	0.0157	chromatin	16	0.0152
cytoskeletal protein binding	25	0.0281	pteridine metabolic process	05	0.0182
learning	07	0.0304	protein pptase 1 reg. activity	03	0.0275
cellular carbohydrate biosynthesis	07	0.0304	chromatin binding	13	0.0312
ribonucleoprotein biogenesis	12	0.0340	apoptosis	37	0.0337
regulation of lipase activity	07	0.0369	phosphoprotein pptase activity	13	0.0361
F-actin capping protein complex	03	0.0375	zinc ion binding	79	0.0386
neurotransmitter secretion	05	0.0385	positive regulation of transcription	28	0.0396
ubiquitin-protein ligase activity	10	0.0403	axonemal dynein complex	03	0.0433
translational initiation	06	0.0435	zinc transmembrane transporter	03	0.0437
			negative reg. developmental process	17	0.0456
			stress-activated protein kinase pathway	07	0.0492